

# STATIONKEEPING MONTE CARLO SIMULATION FOR THE JAMES WEBB SPACE TELESCOPE

Donald J. Dichmann<sup>(1)</sup>, Cassandra M. Alberding<sup>(2)</sup>, Wayne H. Yu<sup>(3)</sup>

<sup>(1)</sup> <sup>(2)</sup> <sup>(3)</sup> Code 595.0, NASA Goddard Space Flight Center, 8800 Greenbelt Road, Greenbelt MD, 20771. 301-286-6621. [Donald.J.Dichmann@nasa.gov](mailto:Donald.J.Dichmann@nasa.gov)

**Keywords:** James Webb Space Telescope, libration point orbit, stationkeeping, Monte Carlo

## ABSTRACT

The James Webb Space Telescope (JWST) is scheduled to launch in 2018 into a Libration Point Orbit (LPO) around the Sun-Earth/Moon (SEM) L2 point, with a planned mission lifetime of 10.5 years after a six-month transfer to the mission orbit. This paper discusses our approach to Stationkeeping (SK) maneuver planning to determine an adequate SK delta-V budget. The SK maneuver planning for JWST is made challenging by two factors: JWST has a large Sunshield, and JWST will be repointed regularly producing significant changes in Solar Radiation Pressure (SRP). To accurately model SRP we employ the Solar Pressure and Drag (SPAD) tool, which uses ray tracing to accurately compute SRP force as a function of attitude. As an additional challenge, the future JWST observation schedule will not be known at the time of SK maneuver planning. Thus there will be significant variation in SRP between SK maneuvers, and the future variation in SRP is unknown. We have enhanced an earlier SK simulation to create a Monte Carlo simulation that incorporates random draws for uncertainties that affect the budget, including random draws of the observation schedule. Each SK maneuver is planned to optimize delta-V magnitude, subject to constraints on spacecraft pointing. We report the results of the Monte Carlo simulations and discuss possible improvements during flight operations to reduce the SK delta-V budget.

## 1. Introduction

The James Webb Space Telescope is a scientific successor of the Hubble Space Telescope and the Spitzer Space Telescope, designed to study and answer fundamental astrophysical questions ranging from the formation of the Universe to the origin of planetary systems and the origins of life. JWST is scheduled to launch in 2018.

JWST will fly in a Libration Point Orbit (LPO) around the Sun-Earth/Moon (SEM) L2 point, with a planned mission lifetime of 10.5 years after a six-month transfer to the mission orbit. Stationkeeping (SK) maneuvers will be performed every 21 days to keep JWST in an LPO around the unstable SEM L2 point. The LPO orbit period is about six months. SK maneuvers are needed to correct for orbit determination errors, maneuver execution errors, uncertainty in Solar Radiation Pressure, and other force modeling errors, as well as momentum unloads (MUs). This paper discusses our approach to SK maneuver planning, the modeling of perturbations, the structure of a Monte Carlo simulation, and the simulation results to determine a conservative SK delta-V budget.

The SK maneuver planning for JWST is made particularly challenging by two factors: JWST has a large, complex, five-layer Sunshield, and JWST will be repointed regularly producing significant changes in SRP. As shown in Figure 6, the effective area of the Sunshield in the Sunward direction can vary between 105 and 163  $m^2$ , for the range of allowed spacecraft attitudes that prevent the telescope from being exposed to stray light. It was therefore important to develop an accurate, attitude-dependent model of SRP. For this we employed NASA Goddard Space Flight Center's (GSFC's) Solar Pressure and Drag tool, which uses ray tracing to accurately compute SRP force and torque as a function of attitude based on a spacecraft model including geometric and reflectivity parameters. The resulting SRP model is also used in JWST's orbit determination analysis, described in a companion paper [1].

As an additional challenge, the JWST observation schedule in the next 21-day period will not be known at the time of SK maneuver planning. A planned observation schedule one week ahead will be available, but the actual observation schedule will be event-driven. If a 'target of opportunity' arises then the schedule can be changed within 48 hours to point at the new target. Also if JWST's Fine Guidance Sensor (FGS) is unable to lock onto a guide star for a scheduled observation, then the observation will be skipped [2]. Thus there can be significant variation in SRP between SK maneuvers, and the future variation in SRP is unknown. To determine an adequate SK delta-V budget, we have enhanced an earlier SK simulation to create a Monte Carlo simulation that includes random draws for orbit determination errors, maneuver execution errors and spacecraft attitude profile. To obtain a conservative SK budget, we modeled the attitude profile using a collection of 190 representative observation schedules developed by the Space Telescope Science Institute (STScI) for JWST. MU schedules provided by STScI were used to drive the simulation. In a separate set of Monte Carlo trials we modeled the attitude profile using 100 randomly-generated (RG) observation schedules, using a uniform distribution of attitude within the constraints of spacecraft pointing. Each SK maneuver is planned to optimize delta-V magnitude, subject to constraints on spacecraft pointing, so that JWST remains in a libration point orbit. The spacecraft is not currently required to follow a pre-determined 'reference' orbit. The additional requirement to follow a specific reference orbit may be necessary for future mission planning, as discussed in Section 10. However, for the current analysis no reference orbit was used and SK maneuvers were only used to keep JWST in orbit around SEM L2.

The remainder of this paper is organized as follows. Section 2 provides a mission overview. Section 3 describes the spacecraft as it relates to SK analysis. Section 4 outlines the algorithm we employ for SK maneuver planning. Section 5 describes the heritage "End-of-Box" analysis our flight dynamics team performed, beginning in 2006. This was a critical step in JWST mission design to provide a conservative but realistic bound on the required SK delta-V budget, before a detailed SRP model was available. Section 6 describes the improved SRP model using SPAD. In Section 7 we outline the attitude modelling used in conjunction with the SRP model to provide a more accurate representation of attitude dependent SRP forces on JWST. In Section 7 we also discuss the Momentum Unload schedules determined by STScI based on the observation

schedule and the spacecraft Center Of Mass (CoM) location. Section 8 describes the structure of the Monte Carlo simulation, which uses random draws of orbit determination error, maneuver execution error, and observation schedule.

In Section 9 we summarize the results of the Monte Carlo simulations. Finally in Section 10 we state the conclusions of this study and planned future work. In particular we discuss possible approaches to improve SRP predictions during flight operations, with the goal to reduce uncertainty in SK planning, so we can reduce the SK maneuver magnitude and perhaps extend mission lifetime.

## 2. Mission Overview

The science goals for the Webb can be grouped into four themes [2], [3]:

1. The End of the Dark Ages: First Light and Reionization seeks to identify the first bright objects that form the early Universe.
2. Assembly of Galaxies will determine how galaxies and dark matter evolved to the present day
3. Birth of Stars and Protoplanetary Systems focuses on the birth and early development of stars and the formation of planets.
4. Planetary Systems and the Origins of Life studies the physical and chemical properties of solar systems, including our own.

The observations needed to accomplish these goals require an infrared telescope. For this, the telescope is cooled to 50 deg K.

To remain passively cooled in a thermally stable environment, JWST will reside far from the Earth in an LPO around SEM L2 point. See Figure 1. In Figure 1 we show the Moon orbit, with semimajor axis 384,400 km, to provide a distance scale: L2 is about four Moon orbit radii, and the LPO width along the y axis is about two Moon orbit radii. JWST is scheduled to launch in 2018 on an Ariane 5 launch vehicle from Kourou, French Guiana. Following launch there will be six-month transfer trajectory including three Mid-Course Correction (MCC) maneuvers that will insert the spacecraft into its mission orbit LPO. For the analysis described in this paper we assume a launch in October 2018 followed by a six-month transfer, so the initial state in the mission LPO is on 20 Mar 2018 at 00:00. The planned duration of science operations in the mission orbit is 10.5 years.

Because the collinear libration points L1 and L2 are unstable, it is necessary to perform regular SK maneuvers to remain in an LPO [4]. For JWST, SK maneuvers are planned every 21 days. For LPO dynamics, it is convenient to describe SK maneuvers in terms of the Rotating Libration Point (RLP) coordinates, where the x-axis points from the Sun toward the Earth/Moon barycenter; the z axis points along the Earth/Moon barycenter orbit normal; and y completed the

orthonormal triad. In this paper, when we refer to the x, y and z axes, it means the RLP x, y and z axes.

In LPO dynamics is known that the x-y plane contains the stable and unstable directions, while the z direction is neutrally stable [5]. Because JWST does not need to remain near a reference orbit, during SK maneuvers there is no need to thrust in the z direction, and the thrust vector is chosen to lie in the x-y plane.

The SK analysis described in this paper is based observation schedules provided by the Space Telescope Science Institute (STScI) using the Science Operations Design Reference Mission (SODRM) 2004 [6]. In the STScI schedules, the spacecraft repoints on average every 5 to 6 hours. Frequent repointing may require Momentum Unload maneuvers, which may induce spacecraft acceleration if the thrust vector does not point through the spacecraft Center of Mass.

## 1. Spacecraft Description

The JWST spacecraft is being built by Northrop Grumman Aerospace Systems (NGAS) and NASA GSFC. As shown in Figure 2, JWST has a large Sunshield designed to block sunlight and other radiation from the Infrared Optical Telescope Element (OTE). The spacecraft bus lies below the Sunshield. The Sunshield provides passive cooling for the OTE, blocking it from both Sunlight and the heat of the bus. The Sunshield has an area about the size of a tennis court, with a maximum Sunward area of  $163 \text{ m}^2$ . As can be seen in Figure 2, the Sunshield has a complex, five-layered structure, blocking the Sun's radiation so the Sun-facing side of the Sunshield has a temperature of 85 deg C, while the OTE is at -223 deg C [2].

The spacecraft body axis J1 points along the OTE boresight; J3 points along the OTE mast; and J2 completes the orthonormal triad. We use a reference spacecraft attitude where the J3 axis points along the RLP x-axis (so -J3 points toward the Sun), the J1 axis points along the RLP y axis, and the J2 axis points along the RLP z axis. In the body frame, the Sun direction is described by two angles: Sun pitch measures the Sun direction from the -J3 axis about the J2 axis, and Sun roll is the Sun direction from the -J3 axis about the J1 axis. (See Figure 4.) Spacecraft pitch and roll angles are the negative of Sun pitch and Sun roll, respectively. The telescope direction is fixed in the body frame, so to point the telescope it is necessary to repoint the entire spacecraft. To prevent sunlight from striking the telescope, the spacecraft attitude is constrained. During SK maneuvers, Sun pitch is bounded between -53 deg to 0 deg, and Sun roll is bounded between -5 deg and +5 deg. During science operations, Sun pitch is bounded between -45 deg to +5 deg. (See Figure 5.)

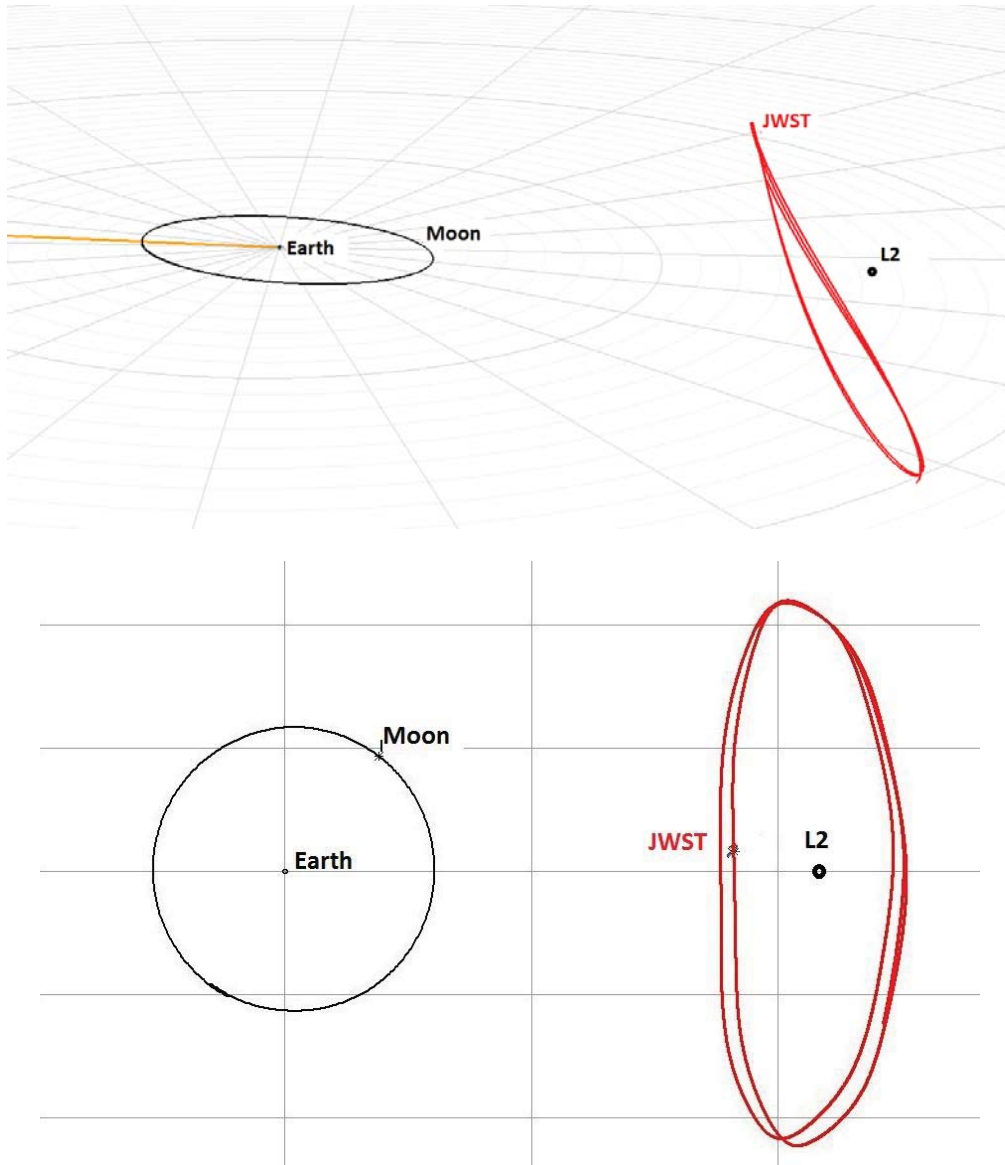


**Figure 1. Plots of the JWST Design Reference Mission LPO about SEM L2. The top plot gives a skew 3D view, while the bottom plot gives a view of the RLP xy-plane. The orange line in the top view is the direction of the Sun from Earth.**

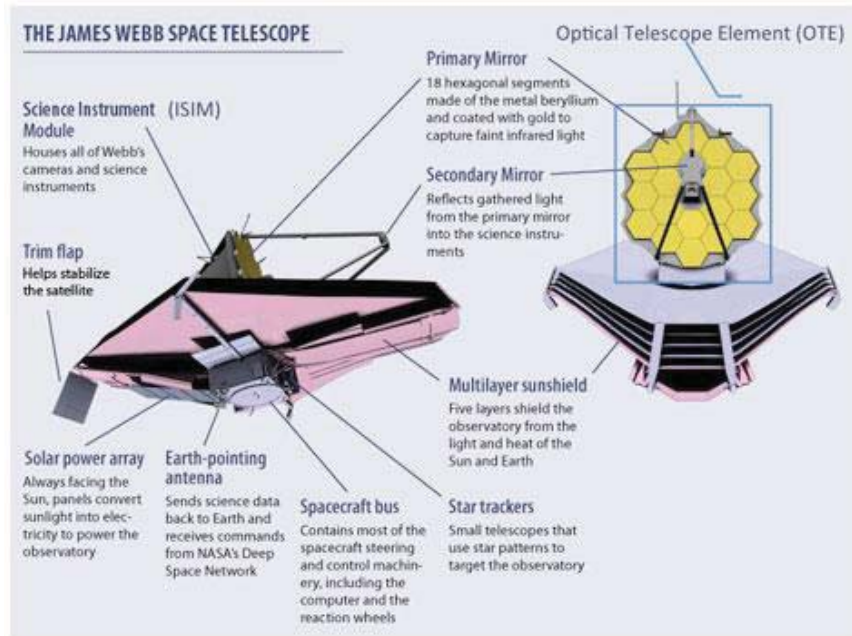


**Figure 2. Diagrams of the JWST spacecraft, showing the large Sunshield, the Optical Telescope Element (OTE), and spacecraft bus below the Sunshield [2] .**

As shown in Figure 3, the thrusters are part of the spacecraft bus and are fixed in the body frame. One set of Secondary Combustion Augmented Thrusters (SCATs) are used for SK and for the final Mid-Course Correction (MCC-2) maneuver. A separate set of SCATs is used for the first two MCC maneuvers (MCC-1a and -1b). The SK SCATs are canted 37.4 deg from the  $-J3$  body axis about the  $J2$  axis. This angle is chosen so the thrust vector will point through the CoM during mission operations. Because the thrust direction is fixed in the body frame, thrusting requires repointing the spacecraft, subject to pointing constraints.

As noted above, LPO dynamics are neutrally stable along the  $z$  axis, and we are not maintaining a pre-determined reference orbit, so there is no need to thrust in the  $z$  direction. During SK maneuvers, JWST will be yawed to place the  $J2$  axis along the RLP  $z$  or  $-z$  axis, so the SK thrust direction is modelled in the RLP  $x$ - $y$  plane. When the  $J2$  axis is along the  $+z$  axis, due to the constraints on pitch angle, the thrust direction is constrained between 37.1 deg and  $37.1 + 53 = 90.1$  deg from the  $x$  axis. (The SCAT thruster is canted at 37.4 deg, as shown in Figure 3. However, it was recommended that we assume a thrust angle of 37.1 deg to correct for plume impingement.) We label this as the Quadrant 1 (Q1) case, although a small part of the angle range extends into Q2. When the  $J2$  axis is along the  $-z$  axis, the thrust direction is constrained between -37.1 deg and -90.1 deg from the  $x$  axis. We label this as the Quadrant 4 (Q4) case.

Note that it is not possible to thrust near the RLP  $-x$  direction. This presents a challenge to JWST maneuver planning during all phases of the mission, in particular during SK if we need to correct for a force modeling error component in the RLP  $+x$  direction. However, as described below, there are ways to cope with this challenge.

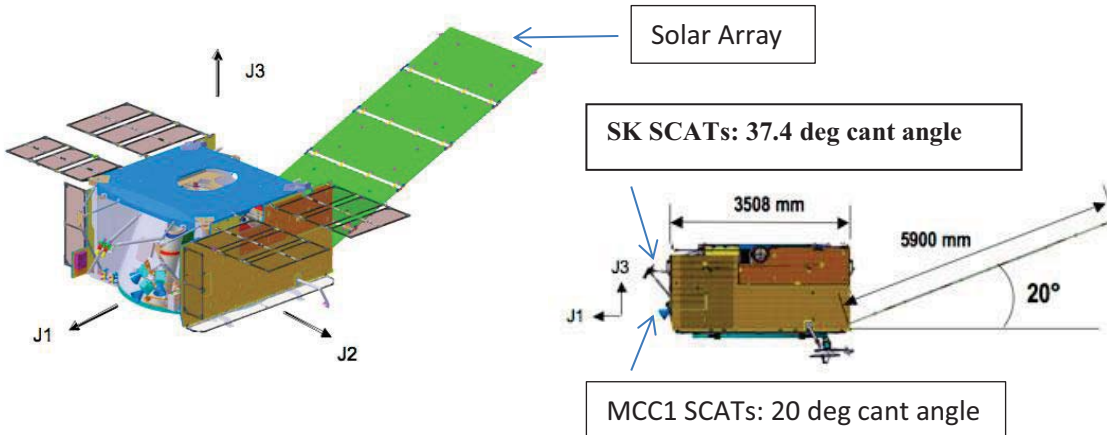


Figure 3. Diagrams of spacecraft bus, including the SCATs [2]. The SK SCATS are canted at 37.4 deg from  $-J3$  toward  $J1$ .

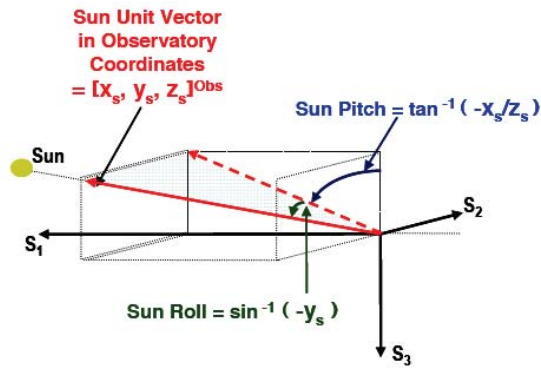


Figure 3-10. Sun Angle Definitions

Figure 4. Definition of Sun pitch and Sun roll angles [7]. The  $S_1$ ,  $S_2$  and  $S_3$  axes are respectively parallel to the  $J_1$ ,  $J_2$  and  $J_3$  axes, with a different origin.



Figure 5. Illustration of the range of pitch angles allowed for JWST during science observations [8].

To achieve the best thruster performance, we were informed by NGAS that it is preferable to only use the SCAT thruster for a maneuver with delta-V above 12 cm/sec. This is another important but manageable challenge in maneuver planning, because a typical SK maneuver is on the order of 12 cm/sec.

## 2. SK Maneuver Planning Algorithm

Because the collinear libration points L1 and L2 are unstable, it is necessary to perform regular SK to remain in an LPO [4]. The SK cost around Sun-Earth/Moon L1 or L2 is about 1 m/s per year, although the exact value depends on the choice of orbit and spacecraft configuration [9]. There have been many studies of the efficient ways to perform SK, some using optimal control techniques and Dynamical Systems Theory, including [10], [11], [12] and the references therein. The SK maneuver planning for JWST presents its own challenges. We cannot choose the time of an SK maneuver; the SK maneuvers are on a regular 21-day schedule. Also, as described above, JWST thrust direction is constrained by the allowed spacecraft attitude.

The SK maneuver planning algorithm is a sequential process, driven by a maneuver schedule provided by STScI that indicates the time for each SK maneuver. The maneuver schedule also indicates the time as well as the delta-V associated with each MU maneuver. The maneuver schedule is an integral part of the observation schedule, which indicates the spacecraft attitude during each visit. All maneuvers are assumed to be impulsive in this analysis. This is considered reasonable because the maneuver magnitudes are small. Each of the 190 available schedules is about 14 months or 420 days long, so it represents events over more than two orbits around L2. (The number and time of the MU maneuvers is different for each schedule, and that affects the duration of the schedule.) Orbit propagation, maneuver modeling and maneuver targeting are performed using Analytical Graphics Inc.'s (AGI's) System Tool Kit (STK)/ Astrogator tool. The SK maneuver planning approach we use for the JWST was described in [13]. The simulation is driven by a Matlab script, which issues STK/Connect and Common Object Module (COM) commands to modify the STK scenario. The simulation starts at an initial state on the LPO. The Matlab script sequentially steps through the STScI maneuver schedule. When an MU maneuver arises in the schedule, the state is propagated until the time of the MU maneuver, and then the MU maneuver is performed. As many as eight MU maneuvers occur between SK maneuvers.

When an SK maneuver arises in the schedule, each 21 days, the script propagates the orbit to the time of the SK maneuver. The script then sets up a targeting problem in STK wrapped inside a constrained optimization problem in the Matlab script. The SK thrust angle is constrained with the range of angles [37.1 deg, 90.1 deg] from the x axis in Q1 case, or [-90.1 deg, -37.1 deg] in Q4 case.

We use the Matlab constrained optimization function *fminbnd* to find the optimal thrust angle for an SK maneuver. For a given thrust angle, the maneuver thrust direction is set in STK/Astrogator. The targeter then determines the thrust magnitude that keeps the spacecraft in a



LPO. Recall that there is no reference orbit to which we try to return; remaining in orbit around L2 is sufficient. This is one reason that JWST’s inability to thrust in near the  $-x$  direction is manageable. We can remain in an LPO with the thrust directions available. The targeting condition used in this simulation is that the trajectory crosses the RLP  $xz$ -plane three times with nearly zero velocity in the  $x$  direction. This crossing condition is typical for LPOs. (See Figure 1, bottom.) When the optimal maneuver has been found, if it is less than 12 cm/sec in magnitude then we do not perform the maneuver, as noted at the end of Section 1.

The effectiveness of an SK maneuver is limited by our knowledge of current state, maneuver execution accuracy and our knowledge of future events. The accuracy of the current state is limited by orbit determination accuracy, which we discuss further below. Because the orbit period is about six months, three crossings span six months (if the SK maneuver is just *before* an  $xz$ -crossing) to nine months (if the SK maneuver is just *after* an  $xz$ -crossing). As noted above, during this maneuver planning phase we do not know the future spacecraft attitude in detail, so we do not know the SRP force in detail. In Section 5 and then in Section 7 we describe the two approaches that have been used to approximate SRP during the planning phase, based on the available SRP model. Also, during the maneuver planning phase we do not know when any future MU maneuvers will occur. We plan SK maneuvers assuming no future MU maneuvers.

After the SK maneuver is planned, we introduce perturbations to represent our uncertainty. We introduce a maneuver execution error, both in magnitude and direction. We introduce a velocity change to represent the error in velocity from orbit determination (OD). We could also introduce a position change, but LPO dynamics are insensitive to a change in position of a few kilometers in OD accuracy, so we do not perturb position. Propagating forward, we change the SRP to represent the attitude the spacecraft would actually fly. Finally, we perform any MU maneuvers that would occur before the next SK maneuver, and then we repeat the SK maneuver planning until the end of the maneuver schedule.

### 3. Heritage “End-of-Box” Modelling

The JWST SK analysis by Janes and Beckman [14] in 2006 employed an “End-of-Box” approach that modeled extreme errors in the uncertainty factors – OD velocity error, maneuver execution error and SRP error - to obtain a conservative but realistic upper bound on the SK delta-V budget. As a foundation for their analysis, Janes and Beckman modeled the velocity and acceleration errors along the three RLP axes and determined that the largest SK delta-V magnitudes are required when the velocity error is along the  $\pm x$  axis. It is significant that the  $x$  axis is the axis closest to the unstable direction SEM L2, which lays 28.6 deg from the  $x$  axis toward the  $y$  axis [15]. (Pavlak [12] also showed that for the Artemis Earth-Moon LPO orbit, the invariant manifolds often lie close to the optimal SK maneuvers.) If the velocity error is along the  $-x$  axis, then results in [14] indicate that the optimal corrective SK maneuver under JWST pointing constraints is the Q1 case. If the velocity error lies along the  $+x$  axis, Janes and Beckman showed that it would be best to correct with a maneuver in Q4 case. In the Q4, Janes

and Beckman showed that the optimal maneuver is near to  $-y$  axis, which is as close as we can get to thrusting along the unstable manifold in Quadrant 3. Janes and Beckman showed that the delta-V cost to correct an error in the  $+x$  direction is higher than the delta-V cost to correct an error of the same magnitude in the  $-x$  direction. This is an important factor in JWST SK: Correcting for a velocity error in the  $+x$  direction is possible, though it costs more than correcting for a velocity error of the same magnitude in the  $-x$  direction.

The End-of-Box approach makes the following assumptions:

1. Each dynamic error is along the  $\pm x$  axis, which is the most expensive direction to correct among the xyz axes.
2. Each dynamic error magnitude is at its extreme.
3. After each SK maneuver, all three dynamic errors point in the same direction, so the errors accumulate.
4. For each SK maneuver, errors in the  $+x$  and  $-x$  direction are equally likely.

For OD error, when the analysis was performed in 2012, the  $3\sigma$  level had been determined to be 2.52 cm/sec [16]. For maneuver execution error, a  $3\sigma$  value of 0.2 cm/sec was assumed, which would be 2% of a typical SK maneuver with magnitude 10 cm/sec. A spherical model is used for SRP. For SRP error, a nominal value of  $A = 200 \text{ m}^2$  was initially used, with a reflectivity coefficient of  $C_R = 1.5$ , so that  $C_R A = 300 \text{ m}^2$ . In later analyses these values were refined: The maximum Sunward area of JWST is  $A = 163 \text{ m}^2$ , and the reflective properties of the five-layer JWST Sunshield imply  $C_R = 1.811$ . However the product  $C_R A$  remained nearly the same at  $295 \text{ m}^2$ . The SRP error was assumed to be 5% of the nominal.

In the End-of-Box approach, for each SK maneuver we first simulate the  $+3\sigma$  errors and solve for the optimal SK maneuver as described in Section 4. We then simulate the  $-3\sigma$  errors and solve for the optimal SK maneuver. It was assumed that the two possibilities are equally likely. Therefore to obtain the representative SK maneuver magnitude, two maneuver magnitudes were averaged. As noted in Section 4, each maneuver schedule close to 420 days long. To get the SK budget for 10.5 years, the simulated delta-V for the observation schedule is multiplied by 10.5 years over the schedule duration, assuming the similar errors throughout the mission lifetime.

The results of the analysis show that the SK delta-V budget for a 10.5 year mission is 25.5 m/sec, or 2.43 m/sec per year. This SK budget is higher than the typical LPO SK budget of about 1 m/sec per year [9], but JWST presents challenges that other LPO missions do not face. The End-of-Box analysis was critical to the JWST mission, because it provided a realistic value for the SK delta-V budget when it was needed to establish a complete spacecraft mass budget.

The results of the End-of-Box analysis provided essential information for JWST mission planning. To have greater confidence in the budget, we decided to make two enhancements to the SK analysis. First, we implemented a more accurate model of SRP that captures the

dependence on spacecraft attitude. Second, we implemented a Monte Carlo simulation to more realistically model the dynamics errors. The improved SRP model, described in the next section, is used in modeling both Stationkeeping in STK/Astrogator and for Orbit Determination in ODTK. The attitude modeling is described in Section 5. The Monte Carlo simulation is described in Section 6.

#### 4. Solar Radiation Pressure Modelling using SPAD

Northrop Grumman Aerospace Systems (NGAS) has provided a detailed model of the spacecraft as well as data tables showing the SRP force as a function of Sun direction [17]. The SRP force has components both along the Sunline and transverse directions, though the dominant component is along the Sunline. Figure 6 shows the Sunline component as a function of Sun direction. In our analysis we normalize the Sunline component, dividing by the SRP pressure magnitude and the reflectivity coefficient 1.811, to quantify the force in units of area. The choice of reflectivity coefficient  $C_R = 1.811$  is based on the optical properties of the Sunshield material, so the maximum normalized force of  $163 \text{ m}^2$  equals the maximum Sunward area. We see from Figure 6 that the normalized force during science operations has a wide range, varying between 105 and  $163 \text{ m}^2$ .

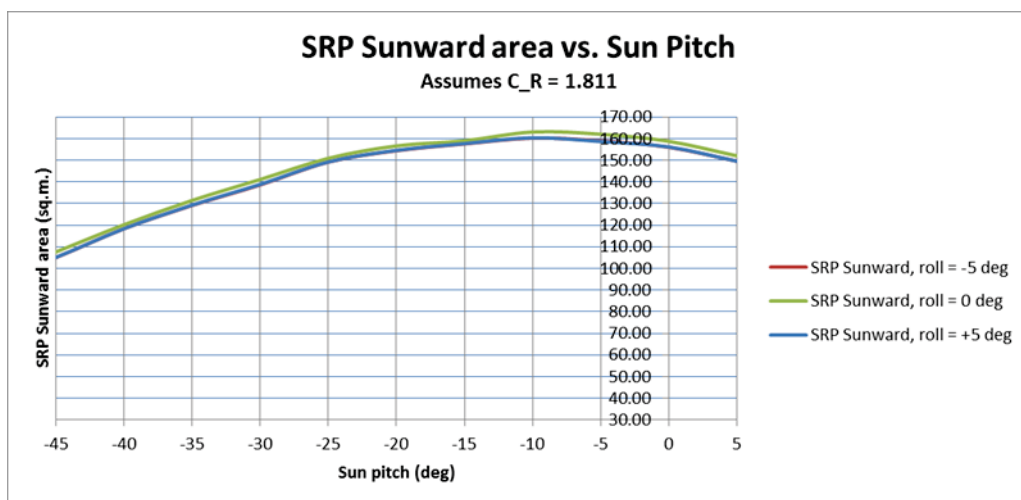


**Figure 6. Plot of SRP Sunward normalized vs. Sun Pitch. Assume reflectivity coefficient of 1.811 [18].**

To enhance the accuracy of our orbit propagation, we decided to develop an SRP model that employs the geometric and reflectivity data in the NGAS spacecraft model. We first considered an N-plate model that had recently been made available by Analytical Graphics Inc. (AGI) for use both in STK and in ODTK [19]. It is important for consistency that we be able to use the same SRP model for both orbit determination and SK analysis, because the two are so closely interrelated. The N-plate plug-in has been used successfully for trajectory analysis on the Mars

Aeronomy and Volatile Evolution (MAVEN) mission, and the trajectory propagation for MAVEN using STK was validated against software at JPL [20]. In an N-plate model, the spacecraft body is modelled by a collection of N plates, each described by the reflectivity parameters, the area and the outward normal in the body frame. The key limitation of the N-plate model is that there is no information about the position of each plate in the body frame, so there is no way to determine if one plate is shadowed by another. For the complex structure on the JWST spacecraft shown in Figure 2, self-shadowing certainly occurs, especially for large pitch angles.

To include attitude dependence and self-shadowing in the SRP model, we decided to employ the NASA GSFC’s Solar Pressure and Atmospheric Drag (SPAD) tool to compute SRP force. As described in the Appendix, SPAD uses a detailed spacecraft model and ray tracing to compute a table of SRP forces as a function of Sun direction. We then modified the AGI N-Plate SRP Plug-in to compute SRP by determining Sun direction and distance at a given time, and interpolating the table of SRP values from SPAD as a function of Sun angles. We could then exploit other features of the AGI plug-in that were unchanged in the SPAD plug-in: To interact with STK to determine the inertial Sun position and the spacecraft attitude, to determine the Sun direction in the body frame, and to convert the SRP force into the inertial frame to be included in orbit propagation. We confirmed that STK was finding the correct attitude from the attitude history file by reporting the attitude and by visualizing the spacecraft attitude in 3D. The SPAD plug-in was validated by reporting the Sun direction in the body frame at several points around the orbit, and confirming the value with a hand calculation. The validation of the SPAD data is discussed in the Appendix. The reuse of much of the plug-in code from AGI, with data from the proven SPAD tool, reduced the software development effort and gave us confidence in the analysis results.

## **5. Attitude Modeling and Momentum Unload Schedule**

There are two distinct phases of SK analysis: SK maneuver planning, and propagation between maneuvers. Attitude for SK maneuver planning is described in Section 5.1, while attitude propagation between maneuvers is described in Section 5.2. Finally in Section 5.3 we discuss Momentum Unloads and the use of Torque Tables.

### **5.1. Propagation between SK Maneuvers**

For this analysis, when we propagate up to the time of an SK maneuver, we assume we know the spacecraft attitude and so are able to model SRP accurately. For one set of Monte Carlo simulations, when we propagate between SK maneuvers we used a collection of 190 observation schedules generated by Wayne Kinzel at STScI. To increase our confidence in the Monte Carlo analysis, for a separate set of Monte Carlo trials we randomly generated (RG) 100 attitude profiles. In the RG profiles

- The attitude changes each 6 hours, much like the STScI schedules.

- During each 6-hour interval the attitude is randomly drawn, with the Sun pitch uniformly distributed between  $-45$  deg and  $+5$  deg, and the Sun roll uniformly distributed between  $-5$  deg and  $+5$  deg. The attitude is held constant during the 6-hour interval.

In flight operations, we will need to plan each SK maneuver a few days before maneuver execution. To fill in the spacecraft attitude during the few days between maneuver planning and maneuver execution, we will be able to use the observation plans that are generated for the next seven days.

## 5.2. SK Maneuver Planning

As noted above, one of the most challenging aspects of SK maneuver planning for JWST is that the observation schedule is event-driven, so we will not have detailed knowledge of the spacecraft attitude more than seven days in the future [6]. Yet when we plan the maneuver, we must propagate six to nine months into the future, and we need to model SRP as accurately as possible during that interval. We considered creating a forward-looking attitude profile, based on the best schedule available, but such a profile would have model hundreds of attitude changes, based on little information. Instead we chose to model the future SRP much as we have previously, by using an elementary spherical SRP model parameterized by the nominal area. This approach allows us to easily vary the nominal area so we can assess how the SK delta-V budget depends on the nominal area.

For our modeling effort, we wanted to confirm that there will be an adequate SK budget if we use a nominal SRP area based on little information about future attitude. If we have no knowledge of the future attitude, other than the pointing constraints, it is reasonable to assume an SRP area in the middle of the ranges of values in Figure 6. For this reason, for most of our Monte Carlo trials we assumed an SRP area of  $140 \text{ m}^2$ . The average area for the STScI schedules, namely  $153 \text{ m}^2$ , differs from the nominal area by  $+9\%$ . The average area for the RG schedules, namely  $120 \text{ m}^2$ , differs from the nominal area by  $-14\%$ . These SRP error magnitudes are respectively 1.8 and 2.8 times the 5% SRP error modeled in the End-of-Box approach.

## 5.3. Momentum Unload (MU) Schedule and Torque Tables

JWST will make frequent attitude changes, and for each repointing the reaction wheels will need to absorb angular momentum. It will be necessary to perform MU thrust maneuvers to unload angular momentum from the reaction wheels. As described in Section 4, each STScI observation schedule is associated with an MU schedule. An MU produces a change in angular momentum delta-H, which induces a change in velocity delta-V if the thrust vector does not pass through the CoM.

To quantify the effects of an error in CoM position, NGAS generated 27 “torque tables”, each corresponding to a CoM displacement relative to the nominal CoM location. A torque table is a matrix that determines the delta-V that would be produced by a delta-H. Each torque table is labeled by a triple of indices  $I_1 I_2 I_3$ , each taking value 1, 2 or 3, so the 27 torque tables are

labelled 111 to 333. Index  $I_n$  tells whether the CoM component along body axis  $J_n$  is (1) at the nominal position; (2) at the positive extreme displacement; or (3) at the negative extreme displacement. For example, torque table 312 corresponds to the case where the CoM component along the  $J_1$  axis is at the negative extreme; the CoM component along the  $J_2$  axis is at the nominal position; and CoM component along the  $J_3$  axis is at the positive extreme. In particular, torque table 111 corresponds to a CoM at the nominal position, so the SCAT thrust passes through the CoM, and an MU would produce no delta-V. The extreme displacement magnitude is based on a sensitivity analysis by NGAS [7]. For the End-of-Box analysis, torque table 222, where all CoM components are at the extreme positive magnitude, was used as the stressing case because it produced the largest SK delta-V budget. It was also noted that Torque Table 22 produced the largest average MU magnitude.

## 6. Structure of Monte Carlo Simulation

For the Monte Carlo simulation we generate the random draws based on Random Stream in Matlab with a fixed seed, to allow repeatability. We also used the Matlab Distributed Computing Toolbox to execute Monte Carlo trials simultaneously on as many as six cores of a single workstation. Distributed computing allowed us to explore more possibilities, and have greater confidence in the results of our statistical analysis. Our implementation of the Monte Carlo simulation was guided by Schiff and Dove's work for the Magnetosphere Multiscale (MMS) mission [21].

For each set of trials, we first specify whether to use attitude profiles from the set of STSci observation schedules or from the RG observation schedule. We specify which torque table to use to determine the MU maneuvers. The choice of attitude profile together with the choice of torque table determines the schedule of Momentum Unloads and their values. As noted in Section 4, the maneuver schedule drives the SK simulation. We also specified the nominal SRP area, typically  $140 \text{ m}^2$ .

For each trial, we first make a random selection of an attitude profile to use as the truth model. For each SK maneuver, we compute the dynamic errors as follows:

- The OD velocity error is based on the covariance. From the most recent OD analysis, the  $3\sigma$  velocity uncertainty is 2 cm/sec, down from 2.5 cm/sec in the End-of-Box analysis [1]. For the velocity covariance, to be conservative, we assumed the same standard deviation of 2/3 cm/sec in each RLP direction. We perform a random draw of a normally distributed 3-vector, and multiply the vector by a square root of the covariance computed with the Cholesky decomposition.
- The maneuver execution error magnitude is modelled as a normally distributed random variable with  $3\sigma$  value of 5%. For the maneuver execution direction error, we assume the cone angle from the nominal direction is normally distributed with  $3\sigma$  value of 4 deg,

based on JWST capabilities. The clock angle around the nominal direction is assumed to be uniformly distributed between 0 and 360 deg.

At the end of each trial, we store a data file describing the maneuvers, a text file that captures the simulation parameters, and the completed STK/Astrogator scenario. As noted in Section 4, each maneuver schedule is about 420 days long. From these results we needed to perform a statistical analysis to obtain an SK budget for 10.5 years or 3840 days. Toward that goal, for each trial we computed the SK budget mean and variance, then scaled these statistics to represent a standardized schedule of exactly 384 days. To assess the equivalent SK budget for 3840 days, we multiple the 384-day mean and variance each by 10, so the 384-day standard deviation is multiplied by  $\sqrt{10} = 3.16$ . Finally, to obtain the 99<sup>th</sup> percentile SK delta-V, we add 3 times the standard deviation to the mean.

## 7. Results of Monte Carlo Simulation

We ran Monte Carlo trials using the randomly-generated observation schedules, assuming an OD velocity error of 2 cm/sec ( $3\sigma$ ) and a nominal SRP area of  $140 \text{ m}^2$ . This was considered the most stressing, realistic case. We first ran a minimum of 18 trials for each of the 27 torque tables to determine which torque tables produce the largest SK budgets. We recognize that the 18 trials are not statistically significant, but these initial trials did point to the three torque tables where we should concentrate our simulation efforts: tables 111, 112 and 113. For each of these torque tables we ran a minimum of 153 trials. The main results are shown in Table 1, from [22]. It was unexpected that torque table 111 would be a stressing case, because that torque table produces no MU's to be corrected. Recall that for the End-of-Box simulations, torque table 222 was the most stressing. However, because we are modeling much larger SRP errors than before, it appears that the MU maneuvers can actually help to correct for SRP errors.

Torque table	SK mean (m/sec)	SK sigma (m/sec)	99 <sup>th</sup> percentile (m/sec)	Number of trials completed
111	20.56	0.69	22.62	1082
112	19.84	0.67	21.83	153
113	20.03	0.72	21.19	332

**Table 1. Results of Monte Carlo trials with randomly-generated observation schedule, Nominal SRP area  $140 \text{ m}^2$  and OD velocity error 2 cm/sec ( $3\sigma$ ), for the three torque tables with the largest SK budget.**

For all of the cases in Table 1, the SK budget is at most 22.62 m/sec. We recognize that this Monte Carlo simulation uses some simplifications, such as modeling maneuvers as impulsive, and the accuracy is limited by the number of trials, so we assigned a Modeling Uncertainty Factor of 10%. Including that uncertainty, the SK budget would be 24.88 m/sec, less than the mission SK budget of 25.5 m/sec found with the End-of-Box approach. This gives us confidence that the SK budget of 25.5 m/sec is sufficient for JWST's 10.5 year mission.

We also ran simulations with the STScI observation schedules, again assuming an OD velocity error of 2 cm/sec ( $3\sigma$ ) and a nominal SRP area of  $140\text{ m}^2$ . The largest SK budget for this case occurred for torque table 111, shown in Table 2. Again, the SK budget with the Modeling Uncertainty Factor is below the 25.5 m/sec allotted budget.

Torque table	SK mean (m/sec)	SK sigma (m/sec)	99 <sup>th</sup> percentile (m/sec)	Number of trials completed
111	17.21	0.89	19.90	132

**Table 2. Results of Monte Carlo trials with STScI observation schedule, Nominal SRP area  $140\text{ m}^2$  and OD velocity error 2 cm/sec ( $3\sigma$ ), for the torque table with the largest SK budget.**

To assess the dependence of SK budget on the OD error, we ran simulations using an OD velocity error of 1.67 m/sec ( $3\sigma$ ), which OD analysis indicated is achievable. For torque table 111 and Nominal SRP area  $140\text{ m}^2$ , we obtained an SK budget of 22.10 m/sec, 0.52 m/sec less than for an OD error of 2.0 m/sec. This indicates that reducing the OD error can reduce the SK required budget, and potentially extend the mission.

In our simulation we did include the condition, mentioned at the end of Section 3, that a planned maneuver that would be smaller than 12 cm/sec would be skipped for efficiency. We found that we can fly the mission successfully, without an impact on the SK budget. In fact, the simulation results indicate that we could skip 48% of the planned SK maneuver, so in most cases an SK maneuver would be performed every 42 days, not every 21 days. We allowed at most one maneuver to be skipped, even if the next SK maneuver would also be smaller than 12 cm/sec. We made this choice for mission safety. If we skipped one maneuver, and then for some reason we could not perform the next maneuver 21 days later, we could end up waiting 63 days between SK maneuvers, presenting a potential risk for an LPO mission.

Finally, we investigated the effect of choosing a nominal SRP area that more accurately reflects the average SRP area of the observation schedule. For example, using the RG observation schedules we know the average SRP is  $120\text{ m}^2$ . Rather than using a nominal SRP area of  $140\text{ m}^2$ , our simulation results indicate that if we could improve the estimate to  $137\text{ m}^2$  then we could achieve an SK budget of 20 m/sec, a reduction of 2.6 m/sec. Since the planned SK budget is 2.43 m/sec per year, that reduction represent more than one year of SK budget. Because the JWST observation schedule is event-driven, it will not be possible to predict the spacecraft attitude in detail far into the future. Nevertheless this result indicates that, if we can improve our prediction of SRP force even modestly, it may be possible to extend the mission by a year or more.

## 8. Conclusions and Future Work

The JWST mission presents several challenges for SK maneuver planning. There is a large, complex Sunshield and there can be large variations in the spacecraft attitude. Because the



observation schedule is event-driven, we cannot anticipate the attitude in detail more than about a week into the future. In addition, constraints on the spacecraft thrust direction prevent us from directly correcting a velocity error in the RLP +x direction. This paper describes the SK maneuver planning algorithm being used for JWST to remain in an LPO about L2, and how we cope with these challenges to assure that there will be an adequate SK budget. The heritage SK planning algorithm used an “End-of-Box” approach to produce a conservative but realistic budget of 25.5 m/sec for the 10.5 years of science observations. We have now enhanced the SK planning tool in two ways. First, we use a Monte Carlo simulation to generate more realistic errors. Second, we use an SRP model that more accurately computes the SRP force as a function of spacecraft attitude. This SRP model is based on NASA Goddard’s Solar Pressure and Atmospheric Drag (SPAD), which uses ray tracing for greater accuracy and can be used for any spacecraft. We have developed an SRP plug-in to STK and ODTK, based on AGI’s N-plate SRP plug-in, that reads and interpolates the SPAD tabular data. Because the SRP model works for both SK modelling and OD analysis, we have enhanced the consistency and accuracy of JWST mission analysis.

We have used the improved SK maneuver planning tool to achieve greater confidence in the JWST SK budget and to expand the analysis. We have simulated the SK maneuver planning with a variety of observations schedules, the full set of torque tables, and different OD velocity uncertainty values. We have also investigated the effect of the accuracy of the predicted SRP area on the SK budget. The results show that a modest improvement in the estimated SRP used in maneuver planning can reduce the required SK delta-V, and perhaps extend the mission lifetime by a year or more.

The STScI staff recently released information about changes in the observation schedule [6]. They expect about four times as many observations as previously planned, which implies much more frequent changes in spacecraft attitude. We may also receive updated torque tables, reflecting better knowledge of the spacecraft CoM location. When more details about these changes are available, we will repeat the SK budget analysis to assess the impact.

The fact that the SK budget depends strongly on our uncertainty in spacecraft attitude, and so spacecraft SRP, encourages us to investigate ways to improve our estimate of SRP for SK maneuver planning. During flight operations, we will work closely with STScI to obtain the best available observation schedules. After several months in the mission orbit, we will see if it is feasible to use past attitude history to improve the estimated, nominal SRP area so we can potentially reduce the SK maneuver magnitudes and perhaps extend mission length.

Finally, as noted above the current analysis did not require that JWST follow a pre-determined reference orbit. However, requirements to observe moving targets within our solar system may make it necessary keep JWST close to a reference orbit [6], [23]. We will be investigating changes in our SK maneuver planning, such as the approach in [11], to efficiently maintain a reference orbit.

## Acknowledgements

Several colleagues at NASA GSFC made this work possible. John Downing shared his expertise with SPAD and generating SRP force tables for JWST. Edwin Dove shared his expertise with distributed computing on MMS. Conrad Schiff shared his experience on JWST analysis, and performed a peer review that helped us to clarify some key points in this paper.. From AGI, Kenny Kawahara and Johnathan Lowe provided the N-plate SRP plug-in software, and helped us to made STK/Astrogator, the SRP plug-in and attitude history files work together.

## Bibliography

- [1] S. Yoon, "Orbit Determination for the James Webb Space Telescope," in *24th International Symposium on Space Flight Dynamics*, Laurel MD, 2014.
- [2] NASA, "James Webb Space Telescope," NASA, [Online]. Available: [jwst.nasa.gov](http://jwst.nasa.gov). [Accessed 10 Mar 2014].
- [3] J. Mather, "The James Webb Space Telescope and Future IR Space Telescopes," in *Space 2004 Conference and Exhibit*, San Diego CA, 2004.
- [4] D. Dunham and R. Farquhar, "Libration Point Missions, 1978-2002," in *7th International Conference on Libration Point Orbits and Their Applications*, Parador d'Aiguablava, Girona, Spain, 2002.
- [5] J. Danby, *Fundamentals of Celestial Mechanics*, Richmond VA: Willmann-Bell, 1998.
- [6] R. Henry, W. Kinzel and M. Jordan, "JWST Scheduling with SODRM 2012, Presented to the JWST AWG," Space Telescope Science Institute, Baltimore MD, 2014.
- [7] W. Kinzel, "JWST Angular Momentum Management with Pass 1 and 2 Torque Tables," Space Telescope Science Institute, Baltimore MD, 2007.
- [8] Space Telescope Science Institute, "James Webb Space Telescope Field-of-View and Sky Coverage," 2014. [Online]. Available: <http://www.stsci.edu/jwst/overview/design/field-of-view>. [Accessed 20 March 2014].
- [9] C. Roberts, "Long Term Missions at the Sun-Earth Libration Point L1: ACE, SOHO and WIND," in *AAS Astrodynamics Specialist Conference*, 2011.
- [10] K. Howell and H. Pernicka, "Stationkeeping Method for Libration Point Trajectories," *J. Guidance, Control and Dynamics*, vol. 16, no. 1, pp. 151-159, 1993.

- [11] T. Pavlak and K. Howell, "Strategy for Optimal, Long-Term Stationkeeping of Libration Point Orbits in the Earth-Moon System," in *AIAA/AAS Astrodynamics Specialist Conference*, Minneapolis MN, 2012.
- [12] D. Folta, T. Pavlak, A. Haapala and K. Howell, "Earth-Moon Libration Point Stationkeeping: Theory, Modeling and Operations," in *1st IAA/AAS Conference on the Dynamics and Control of Space Systems*, Porto, Portugal, 2012.
- [13] M. Beckman and A. Delion, "James Webb Telescope Stationkeeping Analysis," in *AGI User's Conference*, 2003.
- [14] L. Janes and M. Beckman, "Optimizing Stationkeeping Maneuvers for James Webb Space Telescope," in *NASA Goddard Flight Mechanics Symposium*, 2006.
- [15] M. Hechler and J. Cobos, "Herschel, Planck and GAIA Orbit Design," in *7th International Conference on Libration Point Orbits and Their Applications*, Parador d'Aiguablava, Girona, Spain, 2002.
- [16] C. Schiff, "James Webb Space Telescope Mission Critical Design Review [Powerpoint charts]," 2006.
- [17] D. Gidanian, "JWST Solar Torque Modeling," Northrop Grumman Aerospace Systems, Redondo Beach CA, 2008.
- [18] D. Dichmann, C. Alberding and K. Richon, "JWST Stationkeeping Analysis: Monte Carlo Simulation Results," in *JWST Analysis Working Group, Apr 2013*, 2013.
- [19] T. Johnson and V. Coppola, "Solar Radiation Pressure Plugins," Analytical Graphics Inc., 2010.
- [20] D. Folta, Interviewee, *Personal communication on MAVEN mission*. [Interview]. Mar 2013.
- [21] C. Schiff and E. Dove, "Monte Carlo Simulations of the Formation Flying Dynamics for the Magnetospheric Multiscale (MMS) Mission," in *TBD, TBD, TBD*.
- [22] D. Dichmann, C. Alberding and K. Richon, "JWST Stationkeeping Analysis: Monte Carlo Simulation Results," in *JWST Spacecraft Critical Design Review*, 2014.
- [23] K. Gordon, "James Webb Space Telescope Mission Science and Operations Center: Science Operations Design Reference Mission Revision C," Space Telescope Science Institute, 2012.
- [24] M. Ziebart, "High Precision Analytical Solar Radiation Pressure Modelling for GNSS Spacecraft," Ph.D. Dissertation, University of East London, London, 2001.

## Appendix. Solar Pressure and Atmospheric Drag (SPAD) Modeling for JWST

The SPAD tool was developed at NASA Goddard to compute SRP and atmospheric drag for any spacecraft. For JWST, SPAD takes as input a model provided by Northrop Grumman Aerospace Systems (NGAS) that represent the spacecraft surface using hundreds of small triangular plates. Each plate is defined by its optical coefficients (specular reflection, diffuse reflection and absorption), and the coordinates of each vertex in the body frame. The vertex coordinates determine the area of the plate and its outward normal.

SPAD employs ray tracing to compute SRP force and torque. The algorithm is similar to one described in [24]. The user defines a two-dimensional grid to specify a discrete set of Sun directions in the body frame. For JWST, the grid is a set of azimuth and elevation angle measured from the  $-J3$  axis, which nominally points toward the Sun. The user also defines a pixel size. For each Sun ray direction, SPAD generates a pixel array orthogonal to the ray direction. The pixel array acts like a virtual window through which the Sun's rays pass to illuminate the spacecraft. The array is pixel larger than the maximum diameter of the spacecraft and it is positioned between the ray source and the spacecraft. SPAD models a Sun ray passing through each pixel. SPAD determines which, if any, of the triangular plate is struck by the ray, and computes the resulting SRP force and torque vectors for the portion of the plate visible through that pixel. By using ray tracing, only the parts of the spacecraft struck by a Sun ray are included in the SRP calculation. SPAD also accounts for reflection of the ray from one plate onto another. The maximum number of reflections modeled is another a user setting. SPAD then computes the total SRP force and torque by summing over the pixels.

As noted above, the JWST Sunshield consists of five distinct layers. Radiation that is absorbed by one layer is partially reflected by the next layer, so the cumulative effect is that 95% of the radiation is diffusely reflected. To capture this re-radiation, NGAS recommended that the optical coefficients of the Sunshield material be modified so that absorption is decreased to only 5%, and the diffuse reflection is accordingly increased [17].

Ray tracing, with pixilation and multiple reflections, is computationally intensive so modeling parameters must be chosen judiciously to achieve sufficient accuracy with a reasonable computation time. After several tests, for JWST we chose to use an elevation angle step size of 5 deg, an azimuth angle step size of 10 deg, a pixel size of 10 cm, and a maximum of 1 reflection. We also limited the computations to only consider Sun directions in the body frame that are allowed for JWST, which reduced the required computations by a factor of eight.

For validation we compared the SPAD results with tables provided by NGAS that give the JWST SRP force in steps of 10 deg in Sun pitch and 4 deg in Sun roll. At the NGAS grid points, the SRP force computed using SPAD matched the values computed by NGAS to within a few percent, the estimated accuracy of the NGAS values. Moreover the SPAD elevation step size of

5 deg translates into a Sun pitch step size of 5 deg, compared to a 10 deg step size from NGAS, so the SPAD model achieves at least the accuracy of the NGAS model.